

Cite this: *Chem. Commun.*, 2012, **48**, 6244–6246

www.rsc.org/chemcomm

An organometallic approach for ultrathin $\text{SnO}_x\text{Fe}_y\text{S}_z$ plates and their graphene composites as stable anode materials for high performance lithium ion batteries†

Juan Xu,^a Kwonho Jang,^a Jaewon Choi,^a Jaewon Jin,^a Ji Hoon Park,^a Hae Jin Kim,^b Dong-Hwa Oh,^c Joung Real Ahn^{*c} and Seung Uk Son^{*a}

Received 24th February 2012, Accepted 4th May 2012

DOI: 10.1039/c2cc31376f

Through an organometallic approach, ultrathin $\text{SnO}_x\text{Fe}_y\text{S}_z$ plates with ~ 2 nm single layer-thicknesses were obtained and their graphene composites showed very promising discharge capacities of up to 736 mA h g^{-1} and excellent stabilities as anode materials in lithium ion batteries.

Two dimensional (2D) materials have attracted special attention of material scientists due to their unique physical properties.¹ With the recent rise of graphene as new electrode materials,² graphene-like inorganic 2D materials have been intensively studied.^{1–4} For example, ultrathin Bi_2Se_3 ^{1a} and SnSe ^{1b} plates have been prepared and their electrical properties have been reported. Synthetic strategies for 2D inorganic materials can be classified as following. First, if the materials have layered structural motifs,³ they have strong preferences to be grown in two dimensions. Thus, a relatively facile control of their widths and thicknesses resulted in 2D materials. Second, the 2D shape evolution of diverse materials can be kinetically induced using hard or soft templates.⁴ In the latter method, unexpected 2D materials could be discovered through interactions of the surfactants with growing materials.

Graphene has been used as a versatile platform for diverse secondary composite materials.⁵ For example, metal oxide-incorporated graphene showed enhanced photocatalytic activities.⁵ For use as electrode materials in lithium ion batteries, graphene composites of metals, metal oxides and metal chalcogenides have been extensively prepared.⁶ In these composites, graphene increased not only conductivities of materials but also stabilities through a buffering role. For example, although manganese oxide has a poor conductivity for use as electrode materials, its graphene-composites showed enhanced lithium storage capacities.^{6a}

In addition, wrapping iron oxides with graphene sheets enhanced stabilities in insertion and desertion process of lithium ions.^{6b}

Our research group has developed synthetic methods for diverse colloidal 2D nanomaterials including In_2S_3 , TiS_2 , Sb_2S_3 , Cu_{2-x}Se , SnSe_2 , Ga_2O_3 , Rh, and so on.⁷ In our continuous efforts for discovery of new colloidal 2D materials through an organometallic approach,⁸ we found the formation of unexpected ultrathin inorganic materials. In this work, we report the preparation of unprecedented ultrathin $\text{SnO}_x\text{Fe}_y\text{S}_z$ (SOFS) plates from organometallic precursors, their graphene composites and application as anode electrode materials of lithium ion batteries.

Fig. 1a outlines the synthetic route for the used organometallic precursor and the SOFS plates. The precursor, bis(ferrocene-1,1'-dithiolato)tin (FT) was obtained in a single crystal form.⁹ In a typical synthetic procedure of the SOFS plates, the precursor solution was prepared by dissolving the FT in a mixture of well-dried oleylamine and trioctylphosphine (TOP) under argon. The use of TOP was critical to obtain the 2D materials; without the use of TOP, FeS particles were obtained as a sole product. Under argon, the precursor solution was hot-injected into oleylamine at 240 °C. The reaction mixture was stirred for additional 1 hour, then cooled to room temperature and

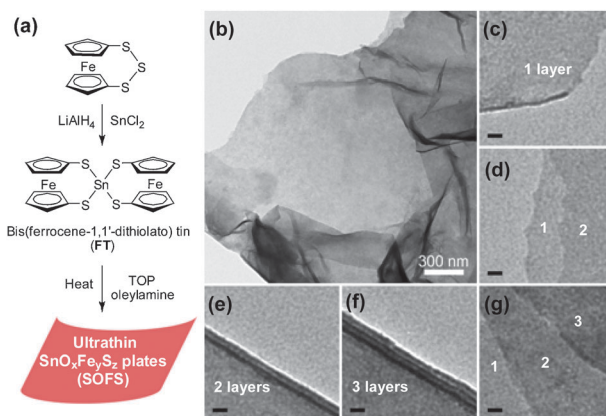


Fig. 1 (a) Synthetic route for the organometallic precursor used in this study and the SOFS plates. (b) TEM image of the SOFS plates; (c) single, (d and e) double, and (f and g) triple layered plates (scale bar in c–g = 10 nm).

^a Department of Chemistry and Department of Energy Science, Sungkyunkwan University, Suwon 440-746, Korea. E-mail: sson@skku.edu; Fax: +82-031-290-4572

^b Korea Basic Science Institute, Daejeon 350-333, Korea

^c Department of Physics and SAINT, Sungkyunkwan University, Suwon 440-746, Korea. E-mail: jrahn@skku.edu

† Electronic supplementary information (ESI) available: Experimental details, additional TEM images, PXRD patterns, XPS spectra and electrochemical characterization of materials. See <http://dx.doi.org/10.1039/c2cc31376f>

poured into excess methanol. The resultant black precipitates were retrieved by centrifugation. After being washed with excess methanol two times, the precipitates were dried under vacuum. The obtained materials were investigated by transmission electron microscopy (TEM).

As shown in Fig. 1b–g and Fig. S1 in the ESI†, the materials have graphene-like 2D shapes. The 2D materials were obtained in the reaction temperature range of 230–260 °C (Fig. S2 in the ESI†). In comparison, irregular FeSn₂ were formed exclusively at 300 °C, indicating that the SOFS plates may be intermediate materials in the formation pathway for iron–tin alloys (Fig. S3 in the ESI†). The optimized synthetic method for the SOFS plates was quite reproducible. Following the optimized experimental conditions above, the SOFS plates of similar quality were prepared 81 times for further studies in our group. The widths of plates were usually observed in the range of 1–5 μm. As shown in Fig. 1c–g, the plates having single, double or several layers were observed. The thicknesses of single layer were measured to be in the range of 1.1–1.9 nm.

The investigation of the chemical components of plates using energy dispersive X-ray spectroscopy (EDS) indicated that the materials consist of Sn, Fe, and S with 2.3:1.9:1.0 stoichiometric ratios respectively (Fig. 2).¹⁰ Powder X-ray diffraction (PXRD) studies showed an amorphous character of materials with only broad peaks at 15–35° (Fig. 3c and Fig. S3 in the ESI†). The high resolution TEM (HR-TEM) analysis

supported an amorphous character of materials (Fig. S4 in the ESI†). Heat-treatment of the isolated plates under argon at 350 °C for 3 hours did not alter the PXRD pattern and shape of plates. X-ray photoelectron spectroscopy (XPS) showed 3d_{5/2} peak of Sn, 2p_{3/2} peak of Fe and 2p peak of S at 486.2, 711.8 and 161.6 eV respectively (Fig. S5 in the ESI†). The positions of these peaks were very close to those of Sn in SnO₂, Fe in FeS and S in FeS respectively; the oxidation states of Sn, Fe and S in materials corresponded to +4, +2, and –2 respectively.¹¹ Considering the stoichiometric ratios among the elements and their oxidation states, it can be speculated that additional anionic element should exist in materials. Through careful analysis of XPS and EDS spectra, we found that a significant amount of oxygen exists in materials. According to 1s peak at 530.6 eV in XPS spectrum, the oxidation state of oxygen corresponded to –2 and was close to O in SnO₂¹¹ (Fig. S5 in the ESI†). To further confirm the existence of oxygen over the materials, the chemical components of materials were analyzed by EDS-elemental mapping.

Fig. 2 shows the homogeneous distribution of oxygen over materials. According to the EDS analysis, the average stoichiometric ratios among Sn, Fe, S and O in five SOFS samples were calculated as 2.3:1.9:1.0:5.4 respectively. Heating the SOFS plates at 500 °C for 3 hours *under argon* resulted in the appearance of diffraction peaks of SnO₂ (JCPDS# 88-0287), further supporting the existence of oxygen in materials (Fig. S6 in the ESI†). The oxide might be incorporated into materials by reaction of ultrathin plates with air. Recently, we reported that ultrathin TiS₂ nanoplates underwent fast exchange of sulfide with oxide by reaction with air.^{7d} We investigated a change in the EDS spectra of the fresh plates upon exposure to air. As the exposure time was increased from 1 hour to 1 day, the ratio of O to S in plates gradually increased from 2.2:1 to 5.4:1, supporting the incorporation of oxide by reaction with air (Fig. S7 in the ESI†).

It is noteworthy that diverse tin or iron-based materials including tin or iron chalcogenides and oxides have been applied as anode materials in lithium ion batteries.^{12,13} In addition, excellent capacities and stabilities of *amorphous* tin oxide-based composite anode materials have been reported.¹⁴ Thus, we applied the amorphous SOFS plates as anode materials in lithium ion batteries. Also, considering the graphene-like shape of SOFS plates, their graphene composites were prepared (Fig. 3a).

In a typical procedure for graphene–SOFS composites, graphene oxide flakes¹⁵ and the SOFS plates were well dispersed in a THF–H₂O (1:1) mixture. Then, hydrazine monohydrate was added to induce reduction of graphene oxides. In control experiments, the SOFS plates were stable and showed no changes in TEM images after treatment with H₂O and hydrazine. The resultant black precipitates were retrieved by centrifugation, washed with acetone and dried under vacuum. TEM analysis of these composites showed the entrapped SOFS plates in the reduced graphene oxide (Fig. 3b). The PXRD studies on the composites showed that packed graphene oxide peaks at 2θ = 10° completely disappeared by reduction (Fig. 3c). In XPS analysis, the Sn 3d_{5/2} orbital peak of graphene–SOFS composites was shifted by ~0.7 eV, compared to that of the SOFS plates.

Using the SOFS plates and their graphene composites, coin-type electrochemical cells were fabricated (See the ESI† for the procedure). For testing the electrochemical performance of cells, they were discharged from open-circuit voltage to 1 mV and then,

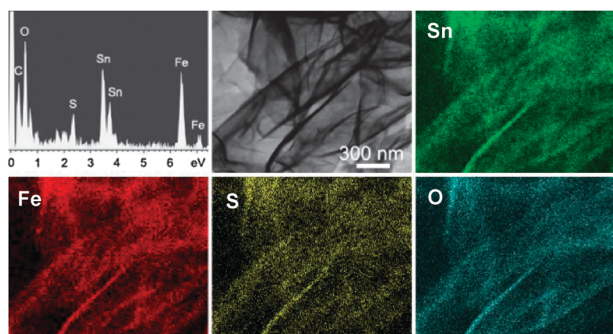


Fig. 2 EDS and EDS-elemental mapping images of the SOFS plates.

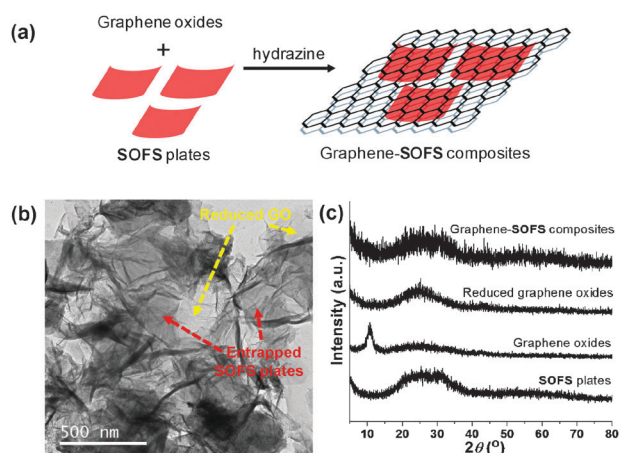


Fig. 3 (a) Cartoon of preparation of graphene–SOFS composites, (b) their typical TEM image, (c) PXRD pattern of the SOFS plates, graphene oxides, reduced graphene oxides and the graphene–SOFS composites.

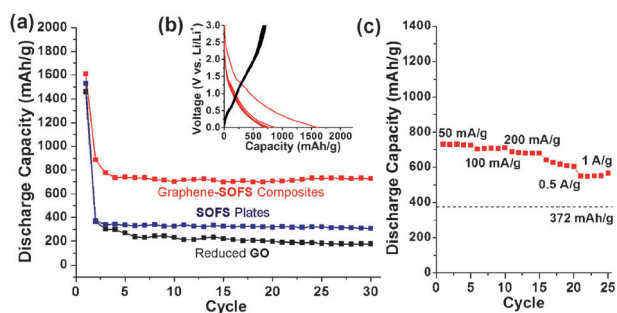


Fig. 4 (a) Discharge capacities of the graphene–SOFS composites with respect to cycling, compared with those of the SOFS plates and reduced graphene oxides (GO); (b) charge (black)–discharge (red) curves and (c) rate performances of the graphene–SOFS composites.

cycled between 1 mV and 3.0 V at a current density of 50 mA g⁻¹. Fig. 4a showed cycle-dependent discharge capacities of materials.

The SOFS plates showed relatively a low discharge capacity of 312 mA h g⁻¹ after 30 cycles, possibly due to low conductivity (Fig. 4a). However, their stability of charge–discharge process was quite surprising. Compared with the discharge capacity of the third cycle, only 23 mA h g⁻¹ was decreased after 30 cycles. The excellent cycling stability of the SOFS plates can be attributed to the possible structural flexibility originated from their *amorphous* character.¹⁶ Enhanced stabilities in *amorphous* materials were reported in Li⁺ insertion of electrochromic metal oxides.^{16b,c}

Graphene composites of the SOFS plates showed quite enhanced discharge capacity and further improved stability. The composites showed 736 mA h g⁻¹ at the fourth cycle and maintained 727 mA h g⁻¹ after 30 cycles (Fig. 4a). It is noteworthy that the reduced graphene oxides without use of the SOFS materials showed 182 mA h g⁻¹ capacity after 30 cycles (Fig. 4a). The mechanical mixture of graphene and the SOFS plates maintained 257 mA h g⁻¹ discharge capacity after 10 cycles. The enhanced capacity and stability of composites might be attributed to the improved conductivity and buffering effect by graphene. In comparison of the cell performance of the graphene–SOFS composites with similar systems in literatures, we found that Honma group recently reported the preparation of graphene–SnO₂ nanocomposites which showed a reversible capacity of up to 810 mA h g⁻¹ in the second cycle and 570 mA h g⁻¹ after 30 cycles respectively.^{12a} In addition, excellent cell performance of tin-based *amorphous* anode materials with 650 mA h g⁻¹ capacity has been reported.¹⁴ Thus, we believe that the capacity and stability (727 mA h g⁻¹ after 30 cycles) of the graphene–SOFS composites in this study are quite promising.

The charge–discharge curves of the graphene–SOFS composites and the SOFS plates show shoulder peaks at 1.3–1.2 V (vs. Li/Li⁺), similar to those of SnO₂-based anode materials reported in the literature¹² (Fig. 4b and Fig. S8 in the ESI†). In addition, it is noteworthy that the voltage (vs. Li/Li⁺) for the reduction process of FeS is known to be 1.33 V.^{13b} As shown in Fig. 4c, the graphene–SOFS composites showed excellent rate performance. They showed 732, 708 and 681 mA h g⁻¹ discharge capacities at the current densities of 50, 100 and 200 mA g⁻¹ respectively. Even at 0.5 and 1 A g⁻¹ current densities, the composites maintained 617 and 553 mA h g⁻¹ capacities, respectively, which are significantly higher than the maximum discharge capacity, 372 mA h g⁻¹ of commercial graphite.

Coulombic efficiencies of the composites reached 97% after 14 cycles and maintained high efficiencies over subsequent cycles (Fig. S9 in the ESI†).

In conclusion, through an organometallic approach, the amorphous SnO_xFe_yS_z plates with 1–5 μm widths and 1.1–1.9 nm thicknesses were obtained. Their graphene composites showed very promising discharge capacities of up to 727–736 mA h g⁻¹, excellent stabilities and columbic efficiencies. This work shows that an organometallic approach can result in formation of the unprecedented nanomaterials for energy applications.

This work was supported by grants NRF-2009-0064488 through the NRF of Korea funded by the MEST. JX thanks for grants NRF-2011-0031392 (Priority Research Centers Program) and R31-2008-10029 (WCU program). HJK thanks for KBSI grants P30402 and Hydrogen Energy R&D Center, a 21st century Frontier Program.

Notes and references

- Selected examples: (a) D. Kong, W. Dang, J. J. Cha, H. Li, S. Meister, H. Peng, Z. Liu and Y. Cui, *Nano Lett.*, 2010, **10**, 2245; (b) D. D. Vaughn, S.-I. In and R. E. Schaak, *ACS Nano*, 2011, **5**, 8852; (c) S. S. Garje, D. J. Eisler, J. S. Ritch, M. Afzaal, P. O'Brien and T. Chivers, *J. Am. Chem. Soc.*, 2006, **128**, 3120; (d) M. B. Sigman, A. Ghezlbash, T. Hanrath, A. E. Saunders, F. Lee and B. A. Korgel, *J. Am. Chem. Soc.*, 2003, **125**, 16050.
- K. S. Novoselov, A. K. Geim, S. V. Morozov, D. Jiang, S. Zhang, V. Dubonos, I. V. Grigorieva and A. A. Firsov, *Science*, 2004, **306**, 666.
- R. Tenne, *Angew. Chem., Int. Ed.*, 2003, **42**, 5124.
- D. V. Talapin, J.-S. Lee, M. V. Kovalenko and E. V. Shevchenko, *Chem. Rev.*, 2010, **110**, 389.
- Review: X. An and J. C. Yu, *RSC Adv.*, 2011, **1**, 1426.
- Recent examples: (a) H. Wang, L.-F. Cui, Y. Yang, H. S. Casalongue, J. T. Robinson, Y. Liang, Y. Cui and H. Dai, *J. Am. Chem. Soc.*, 2010, **132**, 13978; (b) G. Zhou, D.-W. Wang, F. Li, L. Zhang, N. Li, X.-S. Wu, L. Wen, G. Q. Lu and H.-M. Cheng, *Chem. Mater.*, 2010, **22**, 5306.
- (a) J. Choi, J. Jin, I. G. Jung, J. M. Kim, H. J. Kim and S. U. Son, *Chem. Commun.*, 2011, **47**, 5241; (b) K. H. Park, K. Jang and S. U. Son, *Angew. Chem., Int. Ed.*, 2006, **45**, 4608; (c) K. H. Park, J. Choi, H. J. Kim, J. B. Lee and S. U. Son, *Chem. Mater.*, 2007, **19**, 3861; (d) K. H. Park, J. Choi, H. J. Kim, D.-H. Oh, J. R. Ahn and S. U. Son, *Small*, 2008, **4**, 945; (e) K. Jang, H. J. Kim and S. U. Son, *Chem. Mater.*, 2010, **22**, 1273.
- (a) M. L. Kahn, A. Glaria, C. Pages, M. Monge, L. S. Macary, A. Maisonnat and B. Chaudret, *J. Mater. Chem.*, 2009, **19**, 4044; (b) M. Monge, M. L. Kahn, A. Maisonnat and B. Chaudret, *Angew. Chem., Int. Ed.*, 2003, **42**, 5321; (c) J. Xu, K. Jang, J. Lee, H. J. Kim, J. Jeong, J.-G. Park and S. U. Son, *Cryst. Growth Des.*, 2011, **11**, 2707.
- A. Davison and J. C. Smart, *J. Organomet. Chem.*, 1979, **174**, 321.
- The ICP-AES analysis on Sn and Fe showed the 1 : 1.02 stoichiometric ratio of Sn to Fe, which matched well with the EDS results.
- J. F. Moulder, W. F. Stickle, P. E. Sobol and K. D. Bomben, *Handbook of X-ray Photoelectron Spectroscopy*, Phys. Elec. Inc., 1992.
- (a) S.-M. Paek, E. Yoo and I. Honma, *Nano Lett.*, 2009, **9**, 72; (b) J. Fan, T. Wang, C. Yu, B. Tu, Z. Jiang and D. Zhao, *Adv. Mater.*, 2004, **16**, 1432; (c) P. Meduri, C. Pendyala, V. Kumar, G. U. Sumanasekera and M. K. Sunkara, *Nano Lett.*, 2009, **9**, 612.
- (a) B.-C. Kim, K. Takada, N. Ohta, Y. Seino, L. Zhang, H. Wada and T. Sasaki, *Solid State Ionics*, 2005, **176**, 2383; (b) Y. Kim and J. B. Goodenough, *J. Phys. Chem. C*, 2008, **112**, 15060.
- Y. Idota, T. Kubota, A. Matsufuji, Y. Maekawa and T. Miyasaka, *Science*, 1997, **276**, 1395.
- W. Hummers and R. Offeman, *J. Am. Chem. Soc.*, 1958, **80**, 466.
- (a) A. Magasinski, P. Dixon, B. Hertzberg, A. Kvit, J. Ayala and G. Yushin, *Nat. Mater.*, 2010, **9**, 353; (b) P. M. S. Monk, R. J. Mortimer and D. R. Rosseinsky, *Electrochromism and Electrochromic Devices*, Cambridge University Press, 2007; (c) M. Deepa, A. K. Srivastava, S. Singh and S. A. Agnihotry, *J. Mater. Res.*, 2004, **19**, 2576.